

Effects Degrading Accuracy of CPW mTRL Calibration at W Band

G. N. Phung¹, F. J. Schmückle¹, R. Doerner¹, W. Heinrich¹, T. Probst², U. Arz²

¹ Ferdinand-Braun-Institut, Leibniz-Institut für Höchstfrequenztechnik (FBH), Berlin, Germany

² Physikalisch-Technische Bundesanstalt (PTB), Braunschweig, Germany

Abstract—On-wafer measurements of a Device Under Test (DUT) can yield accurate results only if the properties of the measurement environment are well defined and unwanted effects can be removed from the data. This is commonly achieved through a calibration process using a set of different calibration elements. However, various effects may degrade accuracy of this calibration, particularly at higher frequencies. This paper deals with the case of coplanar waveguide (CPW) lines and the multi-line Thru Reflect Line (mTRL) method and discusses two of such issues, the influence of CPW ground width and of probe geometry.

Index Terms—Calibration, measurement accuracy, on-wafer measurement, probe.

I. INTRODUCTION

Any on-wafer measurement data has to be further processed before accurate results for the device under test (DUT) can be obtained. The measured raw data are normally a superposition of various physical effects appearing in the DUT and the region around including neighboring structures on the wafer, the probe and its transition to the pads on the wafer, the wafer material, and the measurement instrumentation itself. All unwanted contributions should be eliminated in a calibration process, in order to obtain the “true” performance of the DUT only. This calibration process is based on a three-step procedure: (i) characterize a set of calibration elements, (ii) calculate error terms from this data, and (iii) use them to correct the raw measurements of the DUT. However, the method needs some basic assumptions on identical conditions for both the calibration standards and the DUT. But as the layout area on a wafer is restricted, the calibration elements often are positioned in a compact way and at different locations on the wafer, thus having different neighboring structures and distances to the wafer edges.

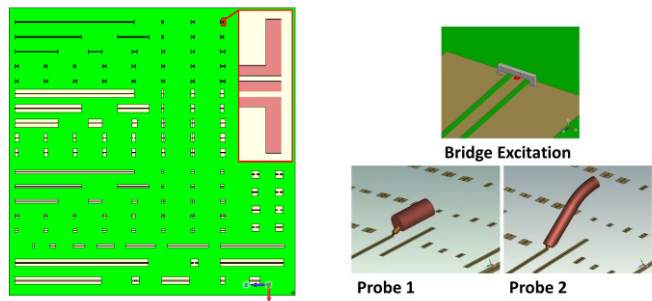


Fig. 1. Layout of the investigated wafer with 3 calibration sets of CPW lines, left: layout, right: different excitations in em simulation.

Several papers [1],[2],[3] have already discussed some of the effects which might influence the accuracy of on-wafer measurements. This paper presents more details for the case of CPW-based measurements up to W band. We study the effects caused by varying CPW ground width and probe geometry and will show which circumstances are usually underestimated and can deteriorate the mTRL calibration and thus accuracy of the results.

II. THE WAFER GEOMETRY INVESTIGATED

The investigations in this paper are based on a layout [1] which was especially designed for the analysis of parasitic effects in calibrations. The substrate (Fig. 1) was manufactured for PTB by Rohde & Schwarz and is referred to as wafer in the following. The material is Al_2O_3 ($\epsilon_r = 9.7$, $\tan \delta = 0.000125$, thickness $625 \mu\text{m}$). The wafer has a rectangular shape and is placed on a thick ceramic chuck ($\epsilon_r = 6.0$, $\tan \delta = 0.02$, thickness $2000 \mu\text{m}$), which emulates a lower open boundary condition in thickness direction. The wafer size is $49 \times 49 \text{ mm}^2$ and the ceramic chuck has a size of $61 \times 61 \text{ mm}^2$. The layout contains, among others, three essentially different sets of CPW calibration elements.

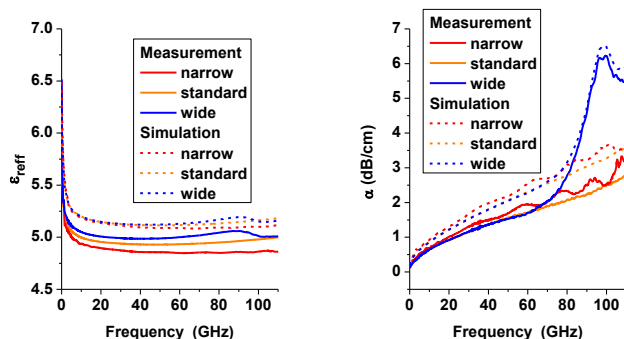


Fig. 2. Propagation constants for CPWs with narrow, standard, and wide ground width.

The common parameters of the CPW lines are an identical signal width of $50 \mu\text{m}$ and $25 \mu\text{m}$ gap with $5 \mu\text{m}$ metal thickness with an assumed conductivity of $\kappa = 35.2 \text{ MS/m}$. What is varied is the ground width of the CPWs, using a ground width of $50 \mu\text{m}$, which is referred to as “narrow” in the following, a ground width of $270 \mu\text{m}$ (“standard”), and a large ground width of $650 \mu\text{m}$ (“wide”). The measurements of the three CPW systems with different ground widths were performed

with GGB probes with a probe pitch of 100 μm . Our calibration set consists of a short and an open as reflects, a 400 μm long CPW line as thru and eight additional lines with lengths of 500, 700, 900, 2400, 5400, 7400, 11400, 20400 μm . Using the calibration elements, we apply mTRL on the raw measured and simulated data for the three different types of CPW systems.

III. PROPAGATION BEHAVIOR FOR DIFFERENT GROUND WIDTHS

For the electromagnetic simulations, Microwave Studio Suite (MWS) from CST was applied [4]. In order to ensure consistency between measured and simulated data, the reference plane was shifted to the probe tips. Furthermore, to include all the effects of a realistic measurement, the simulation of all calibration elements is performed on the complete wafer using a sophisticated probe model (probe 1, see inset in Fig. 1). Fig. 2 presents measured and simulated effective permittivity and attenuation up to W band. One observes a relatively good agreement between simulation and measurements (less than 5% deviation for effective permittivity). Since the details of the measurement probe are unknown and the knowledge of the material properties is limited, some deviations between the measurement and simulations are unavoidable, which document themselves in a slight overall shift between the simulation and measurement curves. It is more important to note that measured and simulated curves exhibit the same peculiarities at certain frequencies. While the CPW with standard ground width shows “typical” CPW characteristics for effective permittivity and attenuation, the CPWs with wide and narrow grounds reveal some discrepancies. The CPW with wide ground width shows the expected behavior up to 80 GHz, but beyond an increase is observed which then turns into a peak at 100 GHz, both in effective permittivity and attenuation. The CPW with a narrow ground, on the other hand, yields a well-behaved characteristic in effective permittivity but strange ripples in the attenuation.

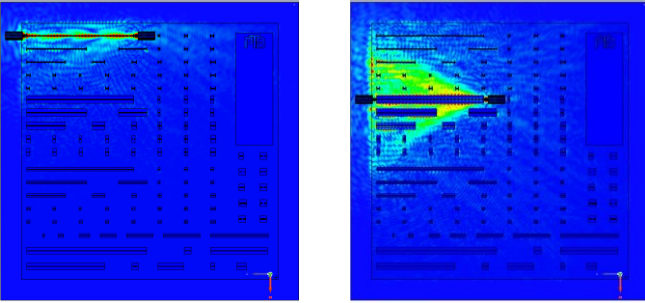


Fig. 3. Field plots: magnitude of the electric field at 100 GHz (top view) for probe 1; left: CPW with narrow ground width; right: CPW with wide ground width (red indicates the strongest and blue the lowest field strength).

Further investigations reveal that the reason for the strong deviation in the wide CPW is the excitation of a higher-order CPW mode, which appears rather early in frequency due to the large total CPW width (Fig. 4) and couples to a substrate

mode outside the CPW. The reason for the ripples in the attenuation of the narrow CPW can be attributed to the special pad structure which differs from the other CPW types. Fig. 3 presents field plots at 100 GHz illustrating these effects. The most critical case is the substrate mode in the wide CPW line (Fig. 4), where a strong part of energy is transferred into the wafer. But also wafer edges and neighboring structures have a clear influence on the fields.

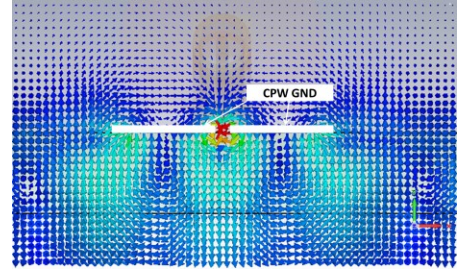


Fig. 4. Field plot shows a higher order CPW mode below the CPW metal and a substrate mode outside excited at 100 GHz for the CPW with wide ground.

IV. COMPARISON OF DIFFERENT PROBES

Another source of deviations can be the use of different probe types. The influence of the probe should be considered in combination with the respective environment close to the tips when contacting the wafer.

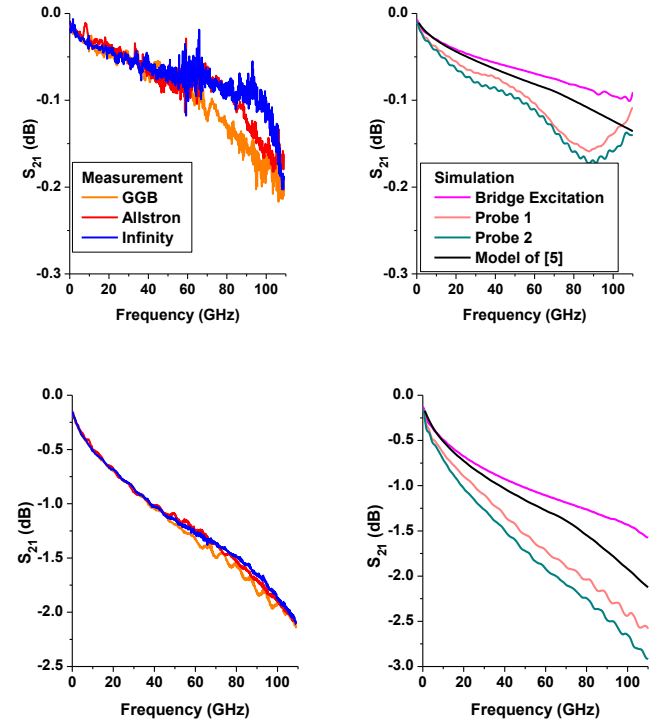


Fig. 5. Calibrated results of the magnitude of S_{21} for the CPW of 500 μm (top) and 7400 μm (bottom) length; left: Measurements with different probes; right: Simulations with different excitations compared to model of [5] (legend shown in top graphs).

In order to investigate the influence of the probes, we performed additional measurements and simulations for the CPW with standard ground width using two other probe types from different manufacturers. In the simulation, we include the complete wafer and excite the DUT with three different models, a simplified bridge model similar to [6] and the two probe versions, probe 1 and probe 2 (see inset of Fig. 1), and compare them with an analytical model of [5]. Probe 1 stands for a geometry with relatively long needles, a thick absorber enclosing the coaxial feeding line, and a straight coaxial extension, oriented in parallel to the wafer. In contrast, probe 2 has a steeper slope of the coaxial extension. This emulates the case where the probe is not parallel to the wafer.

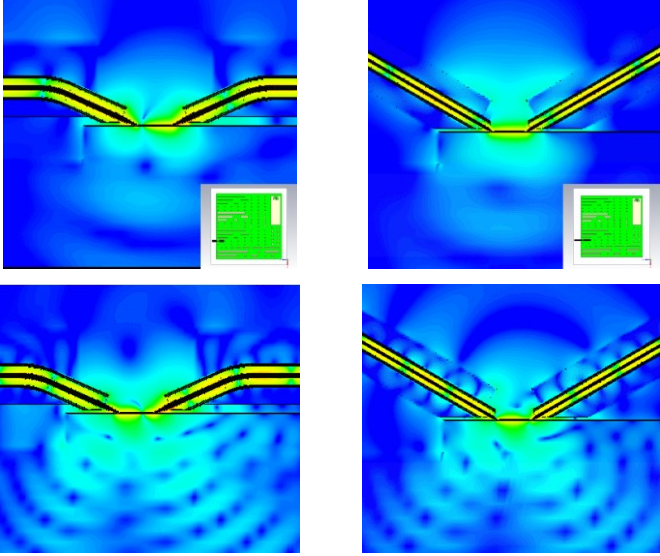


Fig. 6. Field plots: magnitude of the electric field for a 700 μm long CPW excited with different probes; left: probe 1; right: probe 2, top: at 50 GHz; bottom: at 100 GHz.

Although the deviations between the probes do not appear to be very significant, particularly for the short line, Fig. 5 reveals an interesting behavior. The same CPW measured with different probes shows different results, with deviations up to 0.2 dB for the long line (Fig. 5 bottom left). The focus of our investigation is not primarily to determine the maximum deviation; it is to explain how the properties of the probe can change the resulting calibrated data. For a short CPW line of 500 μm length, one normally assumes that the curve behavior would follow a smooth function with a slight increase at higher frequencies comparable to the model of [5] in Fig. 5 (top right). However, the measured calibrated results (Fig. 5 top left) as well as the simulated results with probes 1 and 2 exhibit a wave-like behavior which does not appear at all in model of [5] or the simulation with bridge excitation (least parasitics). The simulation with probe excitation, on the other hand, includes the full parasitics of the probe excitation, i.e., coupling from probe to substrate modes, radiation, and fringing fields between the probe and other structures. This means that the reasons for the unphysical curve behavior can be attributed to the probes, in combination with the calibration

process. The field plots shown in Fig. 6 illustrate the influence of the probe construction (note that the left-hand probe is located at the wafer edge and thus most part extends over air). Fig. 6 shows that depending on the geometry of the probe needles and the absorber construction the fields around the probe transition are distributed differently. The electric fields within the air region below the left-hand probes differ from the fields below the right-hand side probes. Also, the fields in the close vicinity of the CPW and the probe tips differ, as do the fringing fields between the probes, which are clearly higher as in the case of the bridge excitation.

I. REDUCING THE PARASITIC EFFECTS

Both phenomena (radiation depending on the cross section dimensions of the CPW as well as the impact of the probe type) are related to the generation and propagation of substrate modes. The parasitic effects due to the propagation of the substrate mode cannot be completely avoided for this layered system. They are strongly dependent on the permittivities of the chuck material and wafer.

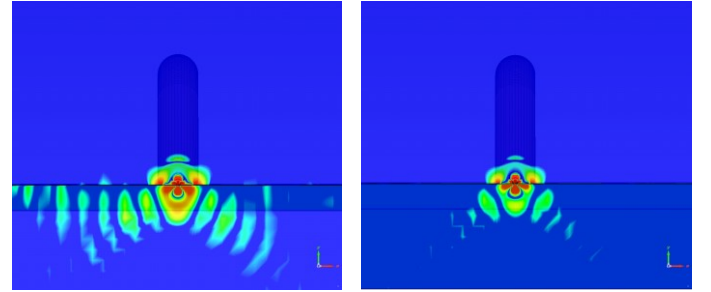


Fig. 7. Vertical electric field component excited with probe 2 at cross section at 100 GHz; left: on ceramic chuck $\epsilon_{r,\text{chuck}} = 6.0$; right: on chuck with same permittivity as the wafer, i.e., $\epsilon_{r,\text{chuck}} = 9.7$. Due to finite discretization cells used in simulation only a moderate resolution of the field representation can be displayed.

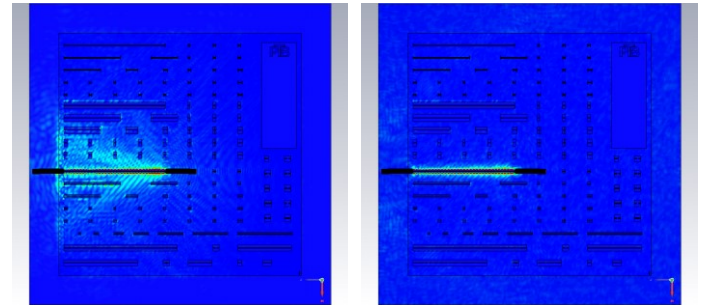


Fig. 8. Field plots: magnitude of the electric field at 100 GHz (top view) excited with probe 2 for nominal CPW ground width; left: on ceramic chuck $\epsilon_{r,\text{chuck}} = 6.0$; right: on chuck with same permittivity as the wafer, i.e., $\epsilon_{r,\text{chuck}} = 9.7$.

E.g., if the wafer is placed on a chuck with same permittivity, the substrate mode vanishes because then wafer and chuck form a homogeneous medium, which does not support a surface wave mode any more. Figs. 7 and 8 support these state-

ments, comparing the vertical electric field component for the CPW line (20400 μm) on different chuck materials. If the chuck permittivity is lower than that of the wafer (here, a ceramic chuck with $\epsilon_{r,\text{chuck}} = 6$ is used), one observes a superposition of radiation effects and propagation of a substrate mode which is generated at probe tips due to the layered structure. Accordingly, in Fig. 8 (left), the electric fields spread over the whole wafer and are reflected back at all discontinuities and edges.

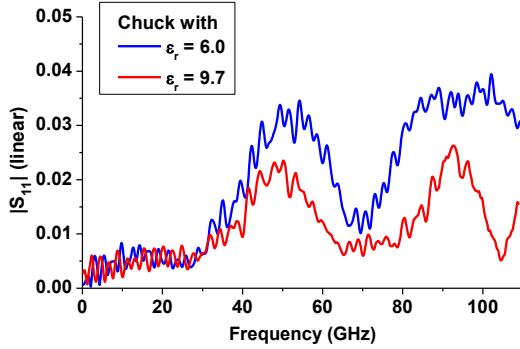


Fig. 9. Calibrated simulation results of the magnitude of S_{11} for the 20400 μm long CPW on different chuck materials.

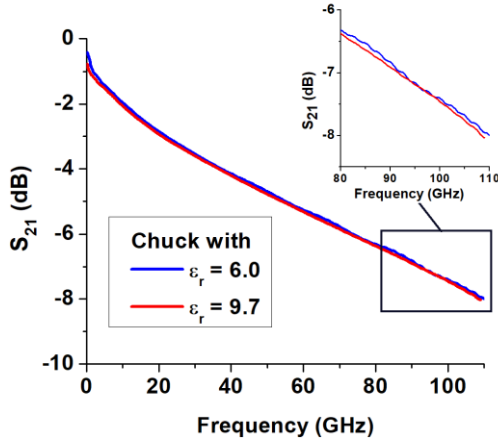


Fig. 10. Calibrated simulation results of the magnitude of S_{21} for the 20400 μm long CPW on different chuck materials.

If the chuck has the same permittivity as the wafer (Figs. 7 and 8, right), the substrate modes are suppressed. Therefore, the lateral spreading fields do not appear anymore and also the reflection coefficient (see Fig. 9) exhibits lower values. This in turn leads to fewer ripple and a smoother curve behavior in the transmission coefficient S_{21} (see Fig. 10). Therefore, using a material for the chuck which has a permittivity value similar to the wafer reduces the effects which contribute to the degradation of the accuracy of CPW mTRL calibrations. Further investigations have shown that this is true for a chuck material with a permittivity larger than that of the wafer, because such a layer structure does not support surface waves either.

II. CONCLUSIONS

Summarizing the results one can state that both effects studied, i.e., the influence of CPW ground width and of probe geometry, are related to the excitation and propagation of substrate modes, which are supported by the 3-layer structure of air, wafer, and ceramic chuck. Thus, the best way to mitigate their impact on calibration accuracy is to suppress them by choosing a chuck with similar or higher dielectric constant than the wafer. Secondly, the cross-sectional dimensions of the CPW elements as well as probe pads have a large impact. An appropriate choice of the design of CPW ground width can avoid parasitic modes. Thirdly, the environment at the probe tips as well as the probe construction itself contributes parasitic effects. So, the vicinity around the probe should be kept free of structures and should be the same for all elements of the calibration set.

ACKNOWLEDGEMENTS

The authors acknowledge support by the European Metrology Programme for Innovation and Research (EMPIR) Project 14IND02 "Microwave measurements for planar circuits and components". The EMPIR program is co-financed by the participating states and from the European Union's Horizon 2020 research and innovation program. The authors are grateful to Rohde & Schwarz for manufacturing the calibration substrate and to Dylan Williams from NIST for providing the initial layout of the substrate.

REFERENCES

- [1] D. F. Williams, F. J. Schmückle, R. Doerner, G. N. Phung, U. Arz, and W. Heinrich, "Crosstalk Corrections for Coplanar-Waveguide Scattering-Parameter Calibrations," *IEEE Trans. Microw. Theory Tech.*, vol. 62, no. 8, pp. 1748-1761, Aug. 2014.
- [2] D. Müller, J. Schäfer, D. Geenen, H. Massler, A. Tessmann, A. Leuther, T. Zwick, and I. Kallfass, "Electromagnetic Field Simulation of MMICs including RF Probe Tips," in *Proc. of the 47th European Microwave Conference (EuMC)*, Nuremberg, Germany, Oct. 2017, pp. 900-903.
- [3] G. N. Phung, F. J. Schmückle, R. Doerner, T. Fritzsch, and W. Heinrich, "Impact of Parasitic Coupling on Multiline TRL Calibration," in *Proc. of the 47th European Microwave Conference (EuMC)*, Nuremberg, Germany, Oct. 2017, pp. 835-838.
- [4] Microwave Studio (MWS) of CST, Darmstadt, Germany.
- [5] W. Heinrich, "Quasi-TEM description of MMIC coplanar lines including conductor-loss effects," *IEEE Trans. Microw. Theory Tech.*, vol. 41, pp. 45-52, Jan. 1993.
- [6] T. K. Johansen, C. Jiang, D. Hadziabdic, and V. Krozer, "EM Simulation Accuracy Enhancement for Broadband Modeling of On-Wafer Passive Components," in *Proc. of the 37th European Microwave Integrated Circuit Conference (EuMIC)*, Munich, Germany, Oct. 2007, pp. 1245-1248.